0022-3565/08/3252-681–690$20.00
THE JOURNAL OF PHARMACOLOGY AND EXPERIMENTAL THERAPEUTICS
Vol. 325, No. 2
132910/3331877
Printed in U.S.A.

JPET 325:681–690, 2008

Preclinical Characterization of Selective Phosphodiesterase 10A Inhibitors: A New Therapeutic Approach to the Treatment of Schizophrenia

C. J. Schmidt, D. S. Chapin, J. Cianfrogna, M. L. Corman, M. Hajos, J. F. Harms, W. E. Hoffman, L. A. Lebel, S. A. McCarthy, F. R. Nelson, C. Proulx-LaFrance, M. J. Majchrzak, A. D. Ramirez, K. Schmidt, P. A. Seymour, J. A. Siuciak, F. D. Tingley III, R. D. Williams, P. R. Verhoest, and F. S. Menniti

Neuroscience, Pfizer Global Research and Development, Groton, Connecticut

Received October 12, 2007; accepted February 15, 2008

ABSTRACT

We have recently proposed the hypothesis that inhibition of the cyclic nucleotide phosphodiesterase (PDE) 10A may represent a new pharmacological approach to the treatment of schizophrenia (*Curr Opin Invest Drug* **8:**54–59, 2007). PDE10A is highly expressed in the medium spiny neurons of the mammalian striatum (*Brain Res* **985:**113–126, 2003; *J Histochem Cytochem* **54:**1205–1213, 2006; *Neuroscience* **139:**597–607, 2006), where the enzyme is hypothesized to regulate both cAMP and cGMP signaling cascades to impact early signal processing in the corticostriatothalamic circuit (*Neuropharmacology* **51:**374–385, 2006; *Neuropharmacology* **51:**386–396, 2006). Our current understanding of the physiological role of PDE10A and the therapeutic utility of PDE10A inhibitors derives in part from studies with papaverine, the only pharmacological tool for this target extensively profiled to date. However, this agent has significant limitations in this regard, namely, relatively poor potency and selectivity and a very short exposure half-life after systemic administration. In the present report, we describe the discovery of a new class of PDE10A inhibitors exemplified by TP-10 (2-{4-[-pyridin-4-yl-1-(2,2,2-trifluoro-ethyl)-1*H*-pyrazol-3-yl]-phenoxymethyl}-quinoline succinic acid), an agent with greatly improved potency, selectivity, and pharmaceutical properties. These new pharmacological tools enabled studies that provide further evidence that inhibition of PDE10A represents an important new target for the treatment of schizophrenia and related disorders of basal ganglia function.

Schizophrenia is a devastating neuropsychiatric syndrome that typically strikes in late adolescence or early adulthood resulting in lifelong disability. Positive or psychotic symptoms, including delusions and hallucinations, are the most apparent manifestation of the disorder. These emerge episodically and usually trigger the first hospitalization in early adulthood. Chronic aspects of the disorder include negative symptoms such as social withdrawal, flattened affect, and anhedonia as well as pervasive cognitive deficits. The latter have been closely linked to a poor function outcome and long-term prognosis (Green, 1996). Psychotic episodes can be controlled, and in many cases prevented, by treatment with dopamine D2 receptor antagonists. These antipsychotic agents represent the first and only line of pharmacotherapy for the treatment of schizophrenia and have significantly reduced the burden of this illness on patients and society. However, the use of antipsychotics can be associated with severe, mechanism-related motor side effects, and 10 to 30% of patients receive little or no benefit from D2 receptor antagonists (American Psychiatric Association, 2004). Although newer, atypical agents with mixed pharmacologies [e.g., D2/5-hydroxytryptamine (5-HT) $_{2A}$ antagonism] have an improved safety profile with respect to motor side effects, many are associated with metabolic effects that can result in serious de novo medical problems (Newcomer, 2005; Mackin et al., 2007). In addition, it is well accepted that neither typical nor atypical agents have meaningful efficacy against the more chronic aspects of schizophrenia, the negative and cog-

Article, publication date, and citation information can be found at http://jpet.aspetjournals.org.
doi:10.1124/jpet.107.132910.

ABBREVIATIONS: 5-HT, 5-hydroxytryptamine; NMDA, *N*-methyl-D-aspartate; PDE, phosphodiesterase; TP-10, 2-{4-[-pyridin-4-yl-1-(2,2,2-trifluoro-ethyl)-1*H*-pyrazol-3-yl]-phenoxymethyl}-quinoline succinic acid; MP-10, 2-[4-(1-methyl-4-pyridin-4-yl-1*H*-pyrazol-3-yl)-phenoxymethyl]-quinoline succinic acid; MK-801, dizocilpine maleate; PCP, 1-(1-phenylcyclohexyl)piperidine (phencyclidine); CAR, conditioned avoidance responding; ANOVA, analysis of variance; AMPH, amphetamine; CREB, cAMP response element-binding protein; pCREB-LI, phospho-CREB-like immunoreactivity; PPI, prepulse inhibition; L-NAME, N^{ω}-nitro-L-arginine methyl ester; HVA, 4-hydroxy-3-methoxyphenylacetic acid.

nitive symptoms (Keefe et al., 2007). Thus, new therapies with improved efficacy in the control of positive symptoms, and the potential to impact cognitive and negative symptoms would provide a significant advancement in the treatment of schizophrenia.

Although the efficacy of D2 receptor antagonists against positive symptoms supports the hypothesis that excessive subcortical dopaminergic activity is an underlying cause of psychosis, the resistance of negative and cognitive symptoms to these treatments implicates other systems in the pathophysiology of schizophrenia. Pharmacological, anatomical, and genetic information indicate that deficits in glutamatergic neurotransmission, particularly mediated by NMDA receptors, may be a contributor to all three symptom clusters (for review, see Coyle, 2006; Javitt, 2007). Although reduced corticostriatal transmission may specifically contribute to an apparent hyperdopaminergia and psychotic symptoms (Laruelle et al., 2003), the downstream consequences of such a disruption may also contribute to the negative and cognitive symptoms of schizophrenia.

It has recently been hypothesized that inhibition of the cyclic nucleotide phosphodiesterase (PDE) 10A will represent a new therapeutic approach to the treatment of schizophrenia (Menniti et al., 2007). PDE10A is highly expressed in medium spiny neurons of the mammalian striatum (Seeger et al., 2003; Coskran et al., 2006; Xie et al., 2006), where it regulates striatal output by its effects on both the cAMP and cGMP signaling cascades (Siuciak et al., 2006a,b; Strick et al., 2006). The hypotheses around the physiological role of PDE10A and the therapeutic utility of PDE10A inhibitors derive in part from studies with papaverine, the only pharmacological tool for this target extensively profiled to date. However, this agent has significant limitations in this regard, namely, relatively poor potency and selectivity and a very short exposure half-life after systemic administration. The present report describes the discovery of a new class of PDE10A inhibitors exemplified by TP-10, an agent with greatly improved potency, selectivity, and pharmaceutical properties. Studies with these new pharmacological tools provide further evidence that inhibition of PDE10A represents an important new target for the treatment of schizophrenia and related disorders of basal ganglia function.

Materials and Methods

Materials. Phencyclidine, amphetamine, risperidone, clozapine, and haloperidol were purchased from Sigma-Aldrich (St. Louis, MO). TP-10 and MP-10 (Verhoest et al., 2006) and ziprasidone were synthesized at Pfizer Global Research and Development.

Compound Administration. TP-10 was dissolved and administered in a vehicle consisting of 5% Emulphor, 5% dimethyl sulfoxide, and 90% saline or 40% β-cyclodextrin. Haloperidol and ziprasidone were dissolved in aqueous 0.3% tartaric acid or 40% β-cyclodextrin, and risperidone was dissolved in aqueous 1.0% glacial acetic acid or 0.3% tartaric acid. All other compounds were dissolved and administered in saline or distilled water (MK-801, PCP). Unless indicated otherwise, all compounds were administered s.c. at doses expressed as the free base in volumes of 10 ml/kg body weight for mice and 1 to 2 ml/kg body weight for rats.

Analysis of TP-10 Concentration in Plasma and Brain. Whole blood was collected via cardiac puncture into microtainer tubes containing Li heparin and centrifuged at 5000 rpm for 2 min; plasma was stored at −80°C. Whole brains were collected via decapitation, rinsed with saline, blotted dry, and stored at −80°C. Brain samples were thawed, diluted 1:4 (w/v) with water, and homogenized using a Kinematica Polytron homogenizer. Standards and controls were prepared in a similar manner using a brain homogenate prepared from untreated animals. Plasma and brain samples (50 μl of standard, control, or sample) were spiked with the internal standard in acetonitrile and centrifuged for 10 min at 3000 rpm. TP-10 concentrations in the supernatant were determined by a reverse-phase high-performance liquid chromatography system using a Phenomenex Primesphere C18 column (30 × 2 mm, 5-μ particle size) and a discontinuous elution gradient (solvent A, 0.1% formic acid and 0.1% isopropyl alcohol in 20 mM ammonium acetate; solvent B, acetonitrile). For TP-10, during the first 0.5 min of the chromatographic run, the mobile phase solvents were held at a constant ratio (95:5, A/B) followed by a 2-min linear gradient to a mobile phase solvent ratio of (10:90, A/B). Retention times for TP-10 were approximately 2.1 min at a flow rate of 0.6 ml/min as monitored by mass spectrometric detection on a Sciex API4000 (MDS Sciex, Concord, ON, Canada) fitted with an electrospray ionization TurboIonSpray interface operated in positive ion mode. Drug and internal standard were analyzed in a multiple reaction monitoring mode using the transitions 461.0 → 143.0 for TP-10. From a ratio of the peak area responses of TP-10 relative to the internal standard, a standard curve was constructed using a linear least-squares regression with a 1/×2 weighting. The lower and upper limits of quantification were 0.5 and 250 or 500 ng/ml, respectively, for each sample source (plasma and brain homogenate).

Enzyme Assays. Phosphodiesterases 1 (A–C), 2A, 3 (A, B), 4 (A–D), 7 (A, B), 8 (A, B), 9A, 10A, and 11 were generated from full-length recombinant clones, PDE5 was isolated from human platelets and PDE6 from bovine retina as described previously (Siuciak et al., 2006b). PDE activity was measured using a scintillation proximity assay. The effect of PDE inhibitors was investigated by assaying a fixed amount of enzyme and varying inhibitor concentrations in the presence of substrate concentrations of one third K_m for each enzyme, such that the IC_{50} approximates the K_i.

Animals. Male C57BL/6J mice (20–30 g) supplied by The Jackson Laboratory (Bar Harbor, ME) were used for the acoustic startle studies, except for the MK-801-disrupted prepulse inhibition studies, which used male CD-1 mice. Male CD rats (250–350 g, locomotor studies), Fisher-344 rats [300–400 g, conditioned avoidance responding (CAR)], and CD-1 mice (20–30 g) supplied by Charles River Laboratories (Kingston, NY) were used for all other studies. Animals were housed under standard laboratory conditions under a 12-h light/dark cycle (lights on at 6:00 AM, 4:00 AM for locomotor rats) with food and water available ad libitum and were allowed a minimum of 1 week for acclimation before experimentation. Animals were handled and cared for in accordance with the Institute of Laboratory Animal Resources (1996), and all procedures were performed with the approval of the Pfizer Institutional Animal Care and Use Committee.

Inhibition of Spontaneous Locomotor Activity. The effect of TP-10 on spontaneous locomotor activity in male CD rats was assessed under conditions associated with high baseline activity (dark cycle) to determine its potential locomotor activity suppressant properties and to evaluate the possible contribution of general behavioral depression to the results obtained in other tests. The locomotor activity boxes consisted of 48 individual Plexiglas behavioral chambers (30 × 30 cm) enclosed in sound-attenuating cabinets. A 24-h timer controlled a single 10-W bulb in each cabinet. The Plexiglas chambers were fitted with grid floors, which were divided into quadrants, and a metal touch plate, which was positioned 7 cm from the floor on all four walls of the chamber. Horizontal locomotor activity is measured as the number of crossovers an animal made from one quadrant to another within its chamber. The test was begun at the onset of the dark cycle (4:00 PM), and the computer was programmed to collect data overnight for a 12-h period. At the beginning of the 12-h dark cycle, male CD rats were administered vehicle or drug at an appropriate pretreatment time. Studies used a 60-min pretreatment time, and animals were returned to their home cage after drug administration. Treatment group means

were compared with a one-way ANOVA followed by Dunnett's test. The ED_{50} values were calculated by linear regression analysis of the dose-response data. Antagonism of PCP- and AMPH-induced hyperactivity TP-10 was tested for its ability to antagonize either PCP- or D-AMPH-induced hyperactivity in rats as described previously (Siuciak et al., 2006b). Male CD rats were habituated in the locomotor chambers overnight before the experiment. The next day, each animal was weighed and treated with either vehicle or drug and immediately returned to the test chamber. After a 60-min pretreatment time, animals were again removed from the test chambers and treated with either PCP (3.2 mg/kg s.c.) or AMPH (1 mg/kg s.c.) and then immediately returned to the test chamber. Horizontal activity (crossovers) was recorded for 3 h after stimulant administration. Treatment group means were compared with a one-way ANOVA followed by Dunnett's test. The ID_{50} values, defined as the dose that produced a 50% inhibition of the vehicle/stimulant treatment group, were calculated by linear regression analysis of the dose-response data using an Excel-based computer curve-fitting program.

Measurement of Striatal Tissue Cyclic Nucleotides. CD-1 mice were sacrificed by focused microwave irradiation of the brain. Regions of interest were isolated and homogenized in 0.5 N HCL followed by centrifugation. Supernatant concentrations of cyclic nucleotides were measured using enzyme immunoassay kits (Cayman Chemical, Ann Arbor, MI). Tissue levels of phospho-CREB-like immunoreactivity (pCREB-LI) were determined by an enzyme-linked immunosorbent assay (BioSource International, Camarillo, CA). Data were analyzed using a one-way ANOVA followed by Fisher's protected least significant difference test with the criterion for significance set at $p < 0.05$.

Measurement of Striatal Cyclic Nucleotides by Microdialysis. Male CD rats were anesthetized with ketamine/xylazine and surgically implanted with guide cannulae in the striatum (A-P, +0.7; M-L, +2.7; D-V, −3.0; Paxinos and Watson, 1986). The cannulae were fixed to the skull with anchor screws and dental cement. At 18 h before the initiation of the experiments, microdialysis probes (4-mm tip; BAS Bioanalytical Systems (West Lafayette, IN) were inserted into the guide cannulae. On the day of the experiments, the probes were continuously perfused with artificial cerebrospinal fluid (NaCl, 147 mM; KCl, 2.7 mM; $CaCl_2$, 1.2 mM; $MgCl_2$, 1.0 mM) at a flow rate of 1 μl/min, and samples were collected every hour into a refrigerated fraction collector. Levels of cAMP and cGMP in dialysates were determined using enzyme immunoassay kits as above. Dialysate concentrations of cGMP and cAMP were normalized to the first four baseline samples.

Catalepsy. Animals were placed in an upright position with forepaws resting on a horizontal bar (9-mm diameter) suspended at a height of 10 cm. The latency to remove the forepaws and climb down to a normal posture was recorded. Animals not responding within 90 s were removed from the apparatus and assigned a latency of 90 s. Animals were tested at 0.5, 1, 2, and 4 h after drug administration. Latencies were ranked within each treatment group for comparison by a Kruskal-Wallace analysis of variance. Post-hoc analyses were performed using Mann Whitney-*U* tests with the criterion for significance set at $p < 0.05$.

Conditioned Avoidance Responding. Testing was performed in rats as described previously (Siuciak et al., 2006b) using commercially available shuttle boxes (Coulbourn Instruments, Allentown, PA). The Plexiglas shuttle boxes were divided by a guillotine door into two sides and enclosed in sound-attenuating chambers. The shuttle boxes were fitted with metal grid floors equipped with scrambled/constant current shockers. Training consisted of repeated 30 pairings of multiple conditioned stimuli of duration (activation of house lights, cue lights, and the opening of the guillotine door), followed 5 s later by a 0.6-mA shock. The shock was terminated when the animal crossed to the other side of the shuttle box or after 10 s. Thirty trials were completed per session, and the number of avoidances (animal crossed before receiving shock, maximum = 30), escapes (animal crossed after receiving shock, maximum = 30), escape failures (animal failed to cross, maximum = 30), latency to avoid (maximum = 5 s), latency to escape (maximum = 10 s), and adaptation crossovers (number of crossovers during a 5-min period before the onset of trials, dark chamber) were recorded by the computer program. The intertrial interval was 30 s in duration, during which time the guillotine door remained closed. Training was continued until a shock avoidance criterion of 80% avoidances was achieved. Compounds were administered 30 min before test sessions. Animals received vehicle treatment 1 day each week, and statistical analyses comparing mean differences in performance under drug to performance under vehicle were tested using paired Student's *t* tests with the criterion for significance set at $p < 0.05$.

Auditory Gating. Experiments were performed as described previously (Krause et al., 2003; Hajós et al., 2005). In brief, male Sprague-Dawley rats (weighing 250–300 g) were anesthetized with chloral hydrate (400 mg/kg i.p.). The femoral vein was cannulated for administration of additional anesthetic and test agents. Anesthetized rats were placed in a stereotaxic frame (David Kopf Instruments, Tujunga, CA), and unilateral craniotomies were performed above the level of the hippocampus. Body temperatures of the rats were maintained at 37°C. Field potentials (electroencephalogram) were recorded from the CA3 region of the left hippocampus, 3.8 mm ventral, 3.5 mm posterior, and 3.0 mm lateral from bregma (Paxinos and Watson, 1986), using a monopolar stainless steel macroelectrode (Rhodes Medical Instruments, Woodland Hills, CA). Data were digitized and stored using the Spike2 software package (Cambridge Electronic Design, Cambridge, UK). Auditory stimulation consisted of two consecutive tone bursts, 10 ms in duration, at a frequency of 5 kHz, delivered through hollow ear bars. Delay between the first "conditioning stimulus" and second "test stimulus" was 0.5 s, and the time interval between tone pairs was 10 s. Auditory evoked potentials were determined by measuring the potential difference between the positive and the negative deflections 20 and 40 ms after stimulation (P20 and N40), respectively. For quantification, 50 sweeps were averaged, amplitudes of auditory evoked potentials were determined, and the level of sensory gating was expressed as percentage of gating: (1 − test amplitude/conditioning amplitude) × 100. D-Amphetamine sulfate (1 mg/kg i.v.) was administered to disrupt sensory gating. TP-10 or its vehicle was applied subsequently, and auditory gating measurements started 5 min after compound or vehicle administration; efficacy was calculated as percentage of reversal of amphetamine-induced gating deficit (percentage reversal). Statistical significance was determined by means of a two-tailed paired Student's *t* test.

Prepulse Inhibition of the Acoustic Startle Response. To evaluate the ability of TP-10 to improve prepulse inhibition of the acoustic startle response C57BL/6J mice were used based on their inherently low level of prepulse inhibition (PPI) (Paylor and Crawley, 1997) and the finding that antipsychotic-induced facilitation of PPI is clearly detected in mice naturally exhibiting poor levels of PPI (e.g., Ouagazzal et al., 2001). In these experiments, compounds were administered s.c., and testing was initiated 30 min after drug administration. To evaluate the ability of TP-10 to antagonize the prepulse inhibition deficits produced by the NMDA antagonist, MK-801, relatively normal-gating CD-1 mice were used. Because the minimal dose of MK-801 that reliably results in a significant disruption of PPI was determined to be 0.178 mg/kg s.c. (data not shown), this dose of MK-801 was administered to mice concurrently with various doses of the test compound, and testing was initiated 30 min later.

Experiments employed eight SR-LAB acoustic startle chambers (San Diego Instruments, San Diego, CA), each consisting of a clear, nonrestrictive Plexiglas cylinder mounted on a platform and housed in ventilated, sound-attenuating external chambers. Placement of mice inside the cylinders allows the whole-body startle responses induced by the acoustic stimuli to be measured via the transduction of movement into analog signals by a piezoelectric unit attached to the platform. A loudspeaker inside each chamber provided continuous background noise and the various acoustic stimuli.

Test sessions consisted of placement of individual animals into the startle chambers and initiation of the background noise (68 dB). After a 5-min acclimation period, each subject was presented with 37 trials in quasirandom order, with randomly varied intertrial intervals (10, 15, or 20 s). The trials consisted of the following types: three no stimulus (i.e., background only), seven startle trials (pulse alone; 40-ms duration; 120 dB), and prepulse-alone trials (20-ms duration; 3, 7, or 9 dB above background; three at each intensity) presented alone or 80 ms before the startle stimulus (prepulse + pulse; 40-ms duration, 120 dB; six at each prepulse intensity). PPI was calculated as a percentage score for each prepulse trial type, and percentage PPI was calculated using the formula: 100 − ((prepulse + pulse)/pulse) × 100. Startle amplitude was calculated as the average response to the seven pulse-alone trials, excluding the first one). Means were statistically compared using ANOVA followed by Dunnett's *t* tests for post-hoc analyses. Data from the no stimulus and the prepulse-alone trials were not included in the analyses because as expected, they elicited only negligible startle responses.

Results

Characterization of TP-10 in Vitro

TP-10 (Fig. 1) inhibited rat recombinant PDE10A in vitro with an IC_{50} of 0.3 nM. The *N*-methyl analog, MP-10 was similarly potent with an IC_{50} of 0.18 nM. Lineweaver-Burke analysis indicated that inhibition is competitive with respect to substrate, and no differences in inhibitory potency were observed when either cAMP or cGMP were used as substrates (data not shown). Both compounds possessed a minimal selectivity of 3000-fold for PDE10A based on IC_{50}s of greater than 1 μM for 18 PDEs representing each of the other 10 PDE families. TP-10 was also analyzed for inhibition of enzyme activity and ligand binding at 80 biologically relevant sites (CEREP panel). The compound exhibited only weak affinity at the following sites (K_i): adenosine A3 receptor (800 nM); leukotriene receptor, LTD4 (1600 nM); and melatonin receptors, ML1 (5100 nM) and ML3 (900 nM). Thus, the minimal selectivity of TP-10 for PDE10A over these other central nervous system drug targets is greater than 2500-fold.

Effect on Cyclic Nucleotides in Vivo

Administration of TP-10 to mice caused a dose- and time-dependent increase in striatal levels of both cGMP and cAMP (Fig. 2, A and B). The absolute magnitude of the elevation of both nucleotides (in picomoles per milligram of tissue) was very similar, as was the dose dependence and time course. Although a definite plateau was not achieved over the dose range evaluated, the results suggest PDE10A inhibition can produce up to a 5-fold elevation in tissue levels of striatal cGMP. The -fold increase in cAMP over basal level was smaller, reflecting the fact that the basal levels of cAMP in the striatum are much higher than those of cGMP. After the administration of a near maximal dose of 3.2 mg/kg s.c., the peak increase in cGMP and cAMP levels occurred between 1 and 3 h, with a return toward control levels by 6 h. Assuming the highest dose of 10 mg/kg results in a maximal response, the ED_{50} for elevating striatal cGMP at 60 min was estimated to be approximately 1.8 mg/kg. Similar results were observed with MP-10. TP-10 was without effect on the tissue cGMP or cAMP levels in the hippocampus and cortex, regions with low levels of PDE10A expression (data not shown).

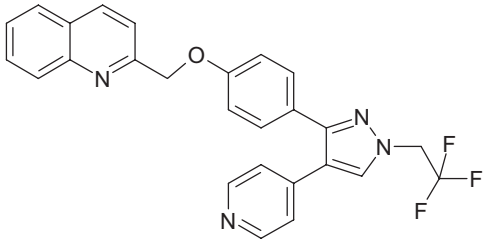

Fig. 1. Structure of TP-10.

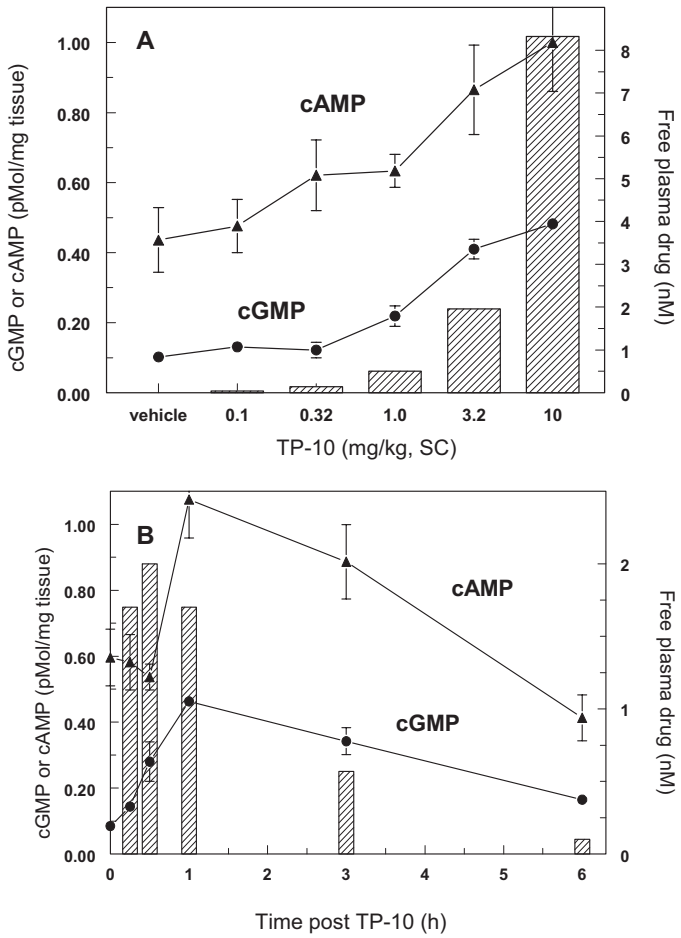

Fig. 2. A, dose-dependent elevation of cAMP and cGMP in mouse striatum 1 h post-s.c. administration of TP-10. Bars, mean free plasma concentrations of TP-10 for each dose at the 1-h time point. B, changes in striatal cAMP and cGMP in the mouse as a function of time after the administration of TP-10 (3.2 mg/kg s.c.). Bars, mean free plasma concentrations of TP-10 at each time point.

Figure 2 also provides the free concentration of TP-10 in plasma for both the dose-response and time course experiments. Changes in striatal cyclic nucleotide concentrations were closely correlated with free concentrations of drug in the plasma. Free plasma TP-10 concentrations associated with a half-maximal increase in striatal cGMP concentrations were estimated to be less than 1 nM, approximating the IC_{50} of the compound for inhibition of PDE10A in vitro (Fig. 2A). Plasma levels of TP-10 reached a maximal level between 0.5 and 1 h after s.c. administration of the 3.2 mg/kg dose (Fig. 2B). At 60 min, the brain (260 ng/g tissue)/plasma concentration (217 ng/ml) ratio was 1.2. A similar tight pharmacokinetic/dynamic relationship was observed for MP-10 (data not shown).

CREB is a transcription factor that is phosphorylated after activation of cyclic nucleotide signaling cascades (Lonze and Ginty, 2002). CREB phosphorylation (pCREB-LI) was deter-

mined in striatal extracts from the dose-response and time course experiments for TP-10 (Fig. 3). The dose-response relationship of striatal pCREB-LI after TP-10 administration paralleled that for cGMP and cAMP (Fig. 3A). However, changes in the pCREB signal occurred more rapidly than those of the cyclic nucleotides (Fig. 3B) and were more closely aligned with plasma drug concentrations than were cyclic nucleotides. Unlike cAMP and cGMP, which peaked at 1 h, striatal pCREB-LI rose within 15 min and peaked at 30 min after the administration of a 3.2 mg/kg dose of TP-10. Furthermore, striatal pCREB-Li had returned to basal levels by 3 h, whereas cyclic nucleotides concentrations were still elevated.

The effect of TP-10 and MP-10 on striatal cyclic nucleotide concentrations were also examined in rats using microdialysis in awake, freely moving animals to confirm our ex vivo observations in mice. Systemic administration of either agent produced significant increases in extracellular concentrations of both striatal cGMP and cAMP. The effect of MP-10 on dialysate concentrations of cAMP and cGMP after a dose of 3.2 mg/kg s.c. is shown in Fig. 4A. In contrast to tissue concentrations of cyclic nucleotides in mice, basal concentrations of cGMP and cAMP in striatal dialysates were similar

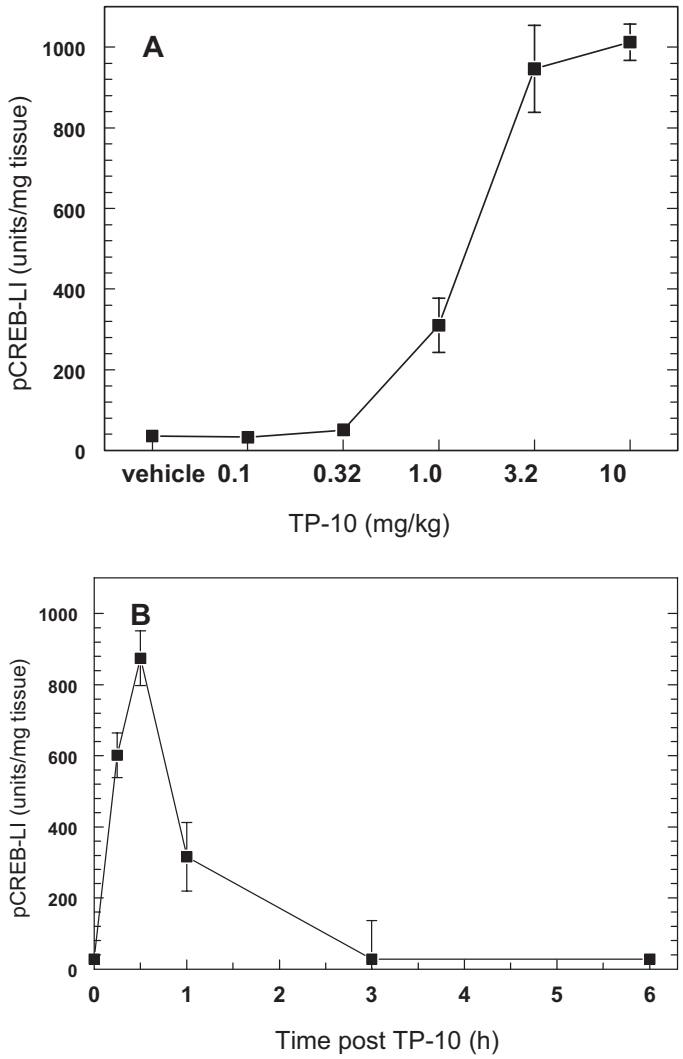

Fig. 3. A, dose-dependent elevation of pCREB-LI in mouse striatum 1 h post-s.c. administration of TP-10. B, changes in striatal pCREB-LI in the mouse as a function of time after the administration of TP-10 (3.2 mg/kg s.c.).

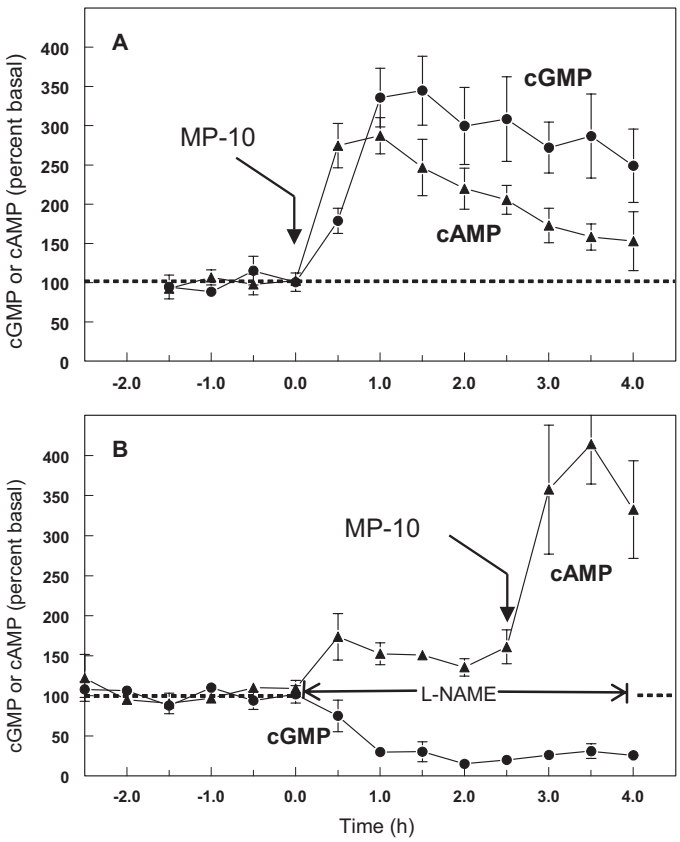

Fig. 4. A, elevation of extracellular cAMP and cGMP in the striatum of awake, freely moving rats after the administration of MP-10 (3.2 mg/kg s.c.). Data are provided as a percentage of baseline using the average concentrations from the first four fractions. B, effect of reverse dialysis with the NOS inhibitor, L-NAME, on the cyclic nucleotide response to MP-10.

(cGMP = 0.039 nM and cAMP = 0.049 nM across four experiments). Extracellular levels of both cGMP and cAMP were increased approximately 3-fold above baseline within 30 to 60 min after the administration of MP-10 and had not fully returned to control levels by the 4-h termination of the experiment. Similar results were observed with TP-10 (data not shown).

To investigate the interdependency of the changes in cAMP and cGMP levels, a second experiment was performed using reverse dialysis of the neuronal nitric oxide synthase inhibitor, L-NAME, to block nitric oxide-induced activation of soluble guanylyl cyclase. As shown in Fig. 4B, infusion of L-NAME (1 mM) produced an immediate decrease in dialysate levels of cGMP and completely inhibited the elevation of cGMP levels after administration of MP-10. In contrast, the elevation of cAMP by MP-10 was unaffected by the infusion of L-NAME.

Effect on DA Turnover

The similarity between some of the behavioral effects of PDE10A inhibitors and D2 receptor antagonists, including a modest cataleptic effect of TP-10 (see below), led to the evaluation of the effect of TP-10 on striatal dopamine turnover. As shown in Fig. 5, TP-10 produced a small, dose-dependent elevation in nucleus accumbens and striatal dopamine turnover as measured by the 3,4-dihydroxyphenylacetic acid + HVA/dopamine ratio.

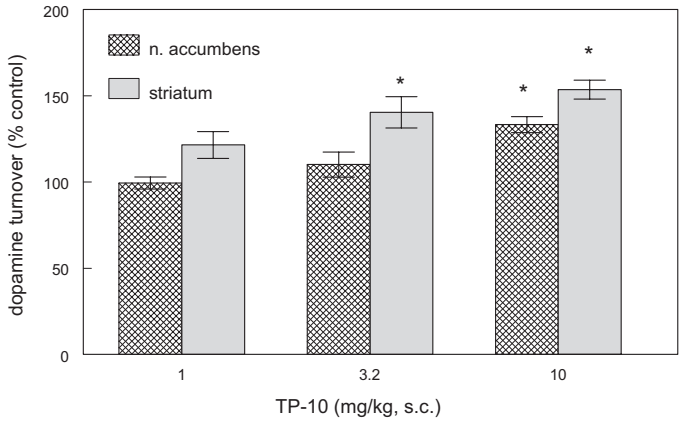

Fig. 5. Dose-dependent elevation of striatal and nucleus accumbens dopamine turnover as measured by the tissue 3,4-dihydroxyphenylacetic acid + HVA/dopamine ratio in rats 1 h postadministration of TP-10.

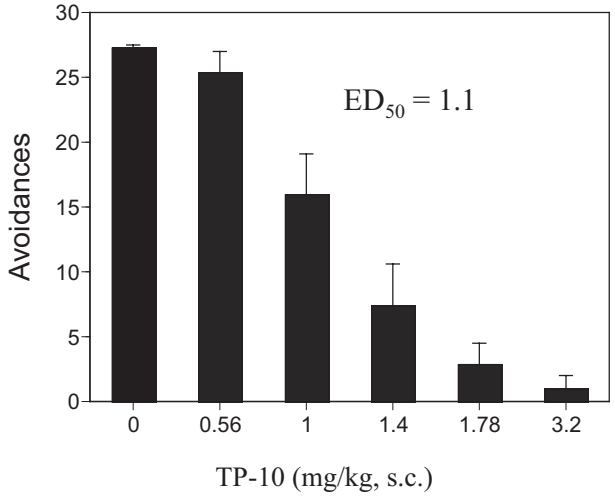

Fig. 6. Dose-dependent disruption of CAR in rats by TP-10. TP-10 was administered 30 min before testing. The ED_{50} in this assay was 1.1 mg/kg. TP-10 did not produce any escape failures over the dose range examined in these studies.

Effects of TP-10 on Behavior

Locomotor Activity. Given the localization of PDE10A in striatal medium spiny neurons and the role of striatum in regulating motor function, the effects of TP-10 on locomotor activity were investigated. TP-10 was administered to rats before introducing the animals to the novel environment of the locomotor activity chambers. Exploratory locomotor activity was reduced in a dose-dependent fashion with an ED_{50} of 1.4 mg/kg (Table 1). TP-10 also produced dose-dependent decreases in PCP- and amphetamine-stimulated locomotor activity, with ED_{50} values of 0.7 and 2.6 mg/kg, respectively (Table 1). The free plasma concentrations of TP-10 associated with these ED_{50} values ranged from 0.6 to 2.2 nM. These values are similar to the free plasma concentrations causing a half-maximal increase in striatal cGMP and cAMP in mice and the EC_{50} for inhibition of PDE10A in vitro. To provide context for these comparisons, the ED_{50} values for inhibition of locomotor activity for several standard antipsychotic agents evaluated under conditions identical to those used for TP-10 are also presented in Table 1.

CAR. Disruption of CAR is a well established preclinical model of antipsychotic activity. An s.c. administration of TP-10 inhibited CAR in rats in a dose-dependent fashion (Fig. 6). The ED_{50} value of 1.1 mg/kg is associated with a free plasma concentration of 1.0 nM. This ED_{50} value is similar to that for inhibition of locomotor activity (Table 1). For comparison, the ED_{50} values for several currently used antipsychotic agents evaluated under identical conditions are presented in Table 1. TP-10 also inhibits CAR in mice, with an ED_{50} value of 2.0 mg/kg s.c. As previously reported for papaverine (Siuciak et al., 2006b), this effect of the compound is absent in mice in which the gene for PDE10A has been disrupted, indicating that the effect of the compound on CAR results from PDE10A inhibition (data not shown).

Hippocampal Auditory Gating in Anesthetized Rats. Recordings of hippocampal field potentials revealed responses evoked by auditory stimuli in anesthetized rats (Fig. 7). As has been reported previously, the second of two evoked responses spaced 0.5 s apart is reduced relative to the first, a process known as auditory gating. Auditory gating can be disrupted by administration of D-amphetamine (1 mg/kg i.v.), as indicated by a significant decrease in the ratio of the test response to the conditioning response (Fig. 7). As shown in Fig. 7, i.v. administration of TP-10 (3 mg/kg; $n = 5$) significantly ($p < 0.05$) reversed the amphetamine-induced gating deficit, whereas administration of the vehicle (1 ml/kg i.v.; $n = 5$) produced no improvement in gating over the same period of time.

PPI of Acoustic Startle. The effect of TP-10 on sensorimotor gating in mice was investigated in two models of PPI, both of which have shown good predictive validity with regard to antipsychotic potential. In C57BL/6J mice exhibiting relatively poor PPI, risperidone (1 mg/kg) significantly increased PPI as shown in Fig. 8A using data collapsed across three prepulse intensities. The effect of risperidone was associated with a statistically significant decrease in startle amplitude (Fig. 8B). In contrast, TP-10 had no effect at any dose at any of the prepulse intensities, nor did the compound reduce startle amplitude (Fig. 8, A and B).

In a second model, CD-1 mice were administered 0.178 mg/kg MK-801 before assessment of PPI. MK-801 significantly reduced PPI from 33.7 ± 3.1 to 14.9 ± 4.4%. Coadministration of risperidone (1 mg/kg s.c.) with MK-801 reversed the MK-801-induced PPI deficit (PPI = 44.4 ± 5.8%). However, TP-10 (1–10 mg/kg s.c.) had no effect on the MK-

TABLE 1
ED_{50} values (milligrams per kilogram s.c.) of TP-10 and standard antipsychotic agents for inhibition of spontaneous (SLA), PCP-stimulated, or amphetamine-stimulated locomotion and CAR

	TP-10 PDE10A	Haloperidol D2	Ziprasidone D2/5-HT2A	Risperidone D2/5-HT2A	Clozapine Atypical
SLA	1.4	0.07	0.71	1.06	1.63
PCP LA	0.69	0.13	0.20	0.15	1.80
CAR	1.1	0.04	0.52	0.13	5.03
AMPH LA	2.6	0.02	0.17	0.07	0.87

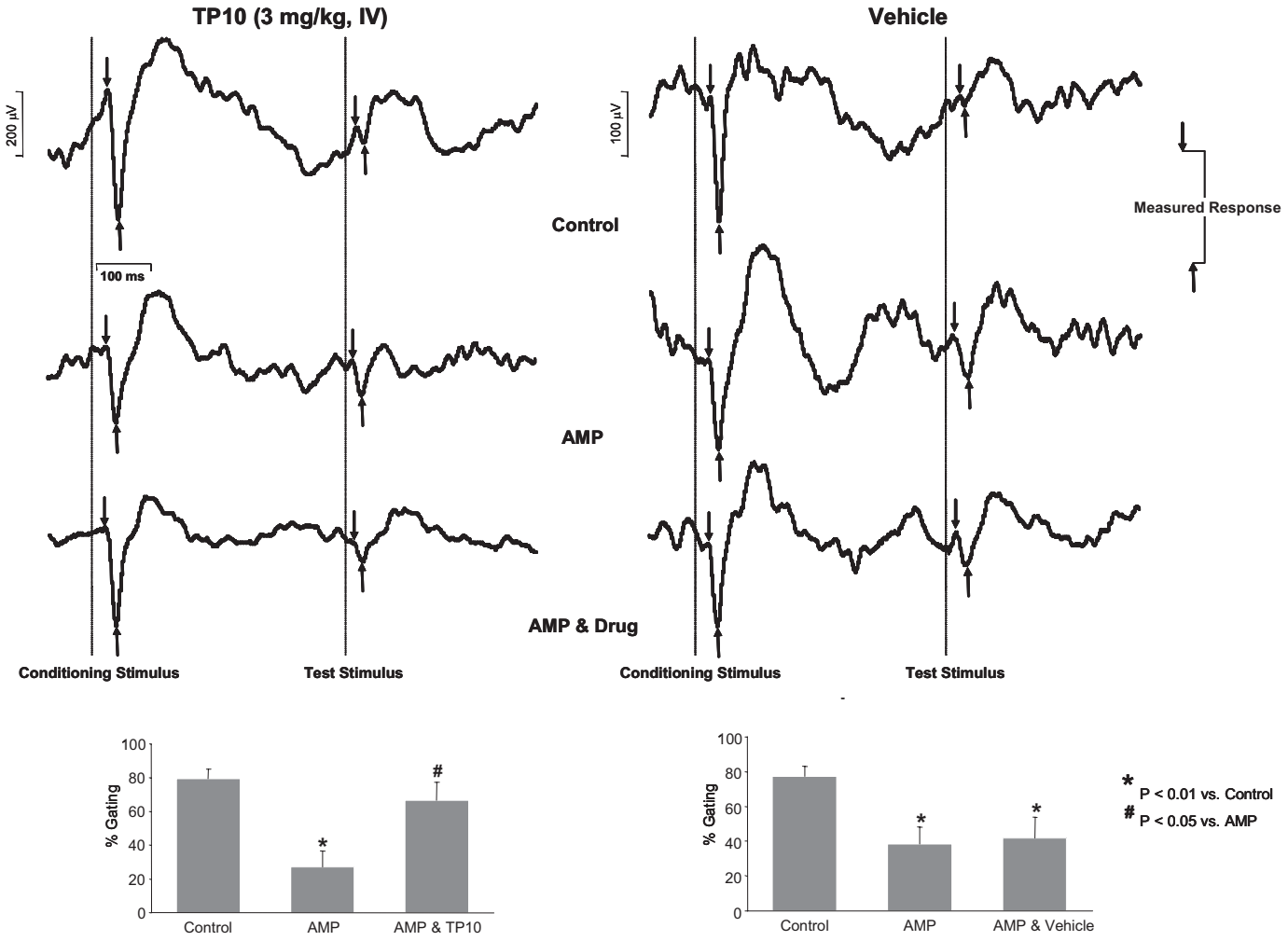

Fig. 7. TP10 improves auditory gating deficits induced by D-amphetamine in anesthetized rats. Typical recordings of hippocampal auditory evoked potentials (summation of 50 consecutive evoked potentials, displayed at a continuous 1-s sweep; upper traces) in response to conditioning and test auditory tones (indicated by dashed lines; intertone interval, 0.5 s) in control conditions (Control) after administration of D-amphetamine (AMP; 1.0 mg/kg i.v.) and after subsequent administration of TP10 (3.0 mg/kg i.v.; left) or its vehicle (right). Arrows, measurement of auditory evoked potential amplitude. Average of hippocampal auditory gating in rats (expressed as a percentage gating, error bars representing SEM; lower panels) during the control period, after D-amphetamine (1.0 mg/kg i.v.), and after subsequent administration of PT-10 (3 mg/kg i.v.; $n = 5$) or its vehicle (1 ml/kg i.v.; $n = 5$). *, $p < 0.01$; #, $p < 0.05$.

801-induced deficit (PPI values ranged from 5.9–18.8% across dose groups).

Catalepsy. The potential of TP-10 to produce motor side effects was assessed by comparing the cataleptic activity of TP-10 to that of the D2 antagonist haloperidol and the D2/5-HT_{2A} antagonist ziprasidone in rats. To meaningfully compare these different agents, each was assessed for the duration of catalepsy as a function of time after drug administration at multiples of the ED_{50} for inhibition of CAR. As shown in Fig. 9A, the degree of catalepsy produced by haloperidol increased as a function of both dose and time. At 2 and 4 h after a dose 30-fold the ED_{50} for inhibition of CAR, essentially all of the animals remained cataleptic through the 90-s cutoff. Although the magnitude of the cataleptic response to ziprasidone was lower than that for haloperidol (Fig. 9B), the pattern of the dose and time dependence was very similar between the two compounds. In contrast, the pattern of the cataleptic response to TP-10 was distinct from that of the D2 receptor antagonists (Fig. 9C). At the lowest multiples of the CAR dose, TP-10 seemed to produce somewhat greater catalepsy than haloperidol or ziprasidone. However, the cataleptic response did not intensify at higher dose multiples or as a function of the time after dosing. Furthermore, the maximal degree of catalepsy produced by TP-10 was less than that produced for either ziprasidone or haloperidol. An identical profile was observed for MP-10 (data not shown).

Discussion

Genetic deletion of PDE10A or inhibition of the enzyme with papaverine has been reported to produce behaviors consistent with increased striatal output (Siuciak et al., 2006a,b). These studies form the basis for the hypothesis that PDE10A inhibitors will have antipsychotic activity in humans (Menniti et al., 2007). Although a useful tool, papaverine has significant limitations in terms of potency, selectivity, and half-life. These limitations have been overcome with a new series of PDE10A inhibitors exemplified by TP-10.

TP-10 competitively inhibited recombinant rat PDE10A with a K_i value of 0.3 nM and possesses a minimum 3000-fold lower affinity for other members of the PDE superfamily. Systemic administration of TP-10 to mice produced an in-

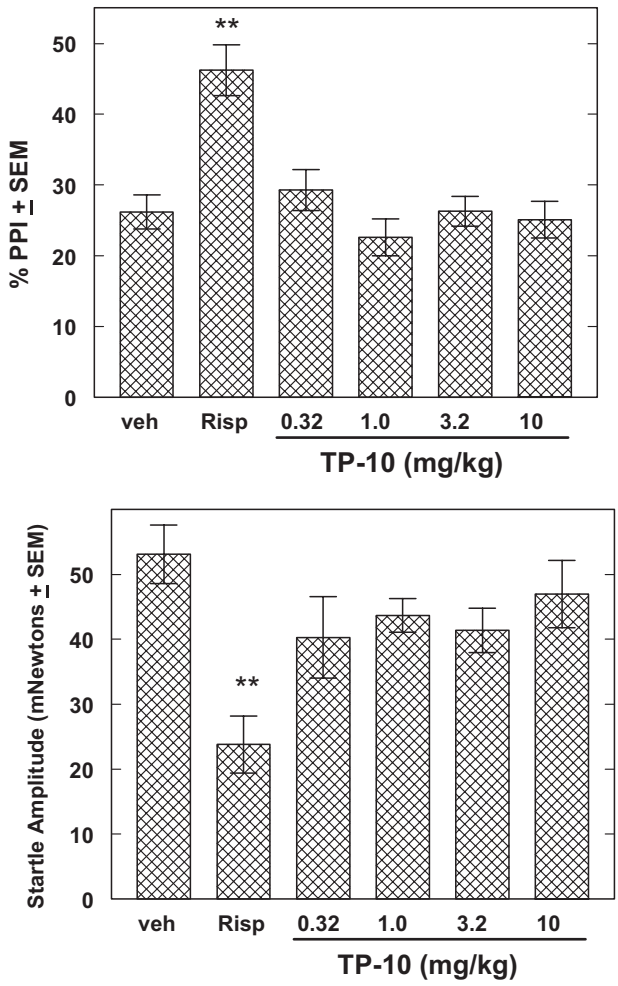

Fig. 8. TP-10 does not improve PPI nor affect startle amplitude in C57BL/6J mice. **, $p < 0.01$ versus vehicle.

crease in tissue concentrations of striatal cGMP and cAMP that closely parallels plasma exposure of the drug. The free plasma concentration of TP-10 associated with the half-maximal increase in striatal cyclic nucleotides approximates the IC_{50} for inhibition of PDE10A in vitro. As predicted by the low levels of PDE10A expression in nonstriatal regions, TP-10 did not increase tissue cyclic nucleotide levels in cerebral cortex or hippocampus.

The hypothesis that PDE10A inhibition will produce an antipsychotic response in the clinic is supported by the behavioral effects of TP-10. In particular, TP-10 reduced exploratory locomotor activity, activity stimulated by the uncompetitive NMDA antagonist PCP, and that resulting from the administration of amphetamine. PCP models a hypoglutamatergic state and is reported to produce behavioral effects similar to the positive, negative, and cognitive symptoms of schizophrenia in humans (Johnson and Jones, 1990; Jentsch and Roth, 1999), whereas amphetamine mimics the hyperdopaminergic state believed to contribute to the generation of psychotic symptoms (see Guillin et al., 2007). Furthermore, TP-10 disrupts CAR, a well established preclinical predictor of antipsychotic activity (Wadenberg and Hicks, 1999) thought to reflect the ability of a compound to reduce stimulus salience (Kapur, 2003). The ED_{50} values for activity in these models are similar to those for increasing striatal levels of cyclic nucleotides.

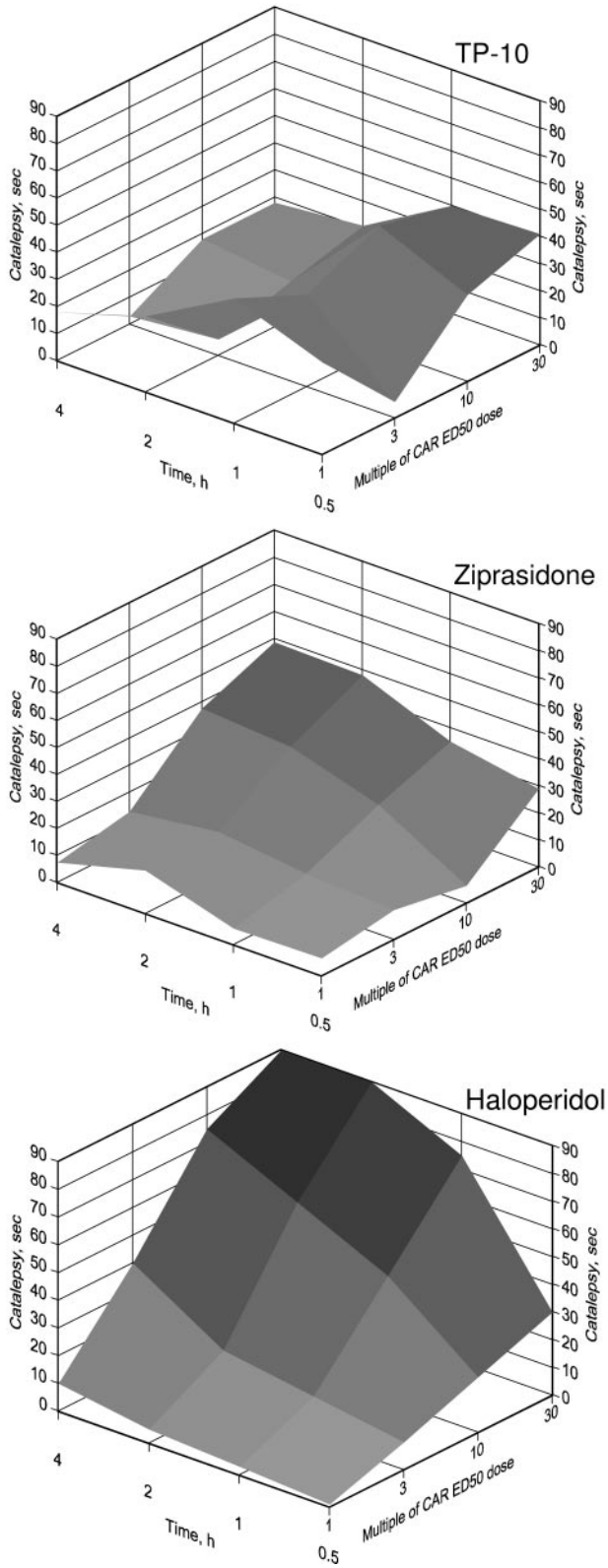

Fig. 9. Cataleptic activity of TP-10, ziprasidone, and haloperidol as a function of dose and time. Each compound was administered as a 1, 3, 10, or 30 multiple of its ED_{50} in CAR, and catalepsy was assessed at 0.5, 1, 2, and 3 h.

Gating deficits may be an endophenotype of schizophrenia (Gottesman and Gould, 2003) and are regarded as one manifestation of the impaired filtering and inefficient processing of sensory information that ultimately lead to perceptual and

cognitive dysfunction (Braff and Light, 2004). The effects of TP-10 on auditory gating deficits were modeled by measuring P50-relevant evoked potentials in response to paired auditory stimuli in the hippocampal CA3 region of anesthetized rats treated with amphetamine. The administration of amphetamine (1 mg/kg i.v.) results in a significant reduction in auditory gating in both the hippocampus and entorhinal cortex. In particular, amphetamine administration diminishes the amplitude of the evoked potential to the first (conditioning) stimuli and enhances the amplitude of the evoked potential to the second (test) stimuli. As previously demonstrated for the D2 antagonist, haloperidol (Krause et al., 2003) TP-10 administered (3.0 mg/kg i.v.) reduced the effect of amphetamine on auditory gating in the CA3 hippocampus. A qualitatively similar effect in the entorhinal cortex did not reach statistical significance (data not shown). In contrast to the results in auditory gating, TP-10 was found to be without effect in two murine models of sensorimotor gating confirmed to be responsive to D2 receptor antagonist, risperidone (Geyer et al., 1990, 2001). In particular, TP-10 did not alter a strain-specific PPI deficit in C57BL/6J mice, nor did it improve PPI in CD-1 mice administered the NMDA antagonist MK-801. Given its similarity to D2 antagonists in a range of neurochemical and behavioral models, the failure of TP-10 to affect PPI was an unexpected observation. In weighing this observation, it is worth noting that mGluR2/3 agonists have also been reported to be inactive against the disruption of PPI by NMDA antagonists (Henry et al., 2002; Imre et al., 2006), yet results from a recent phase II study of the mGluR2/3 agonist prodrug, LY2140023, report antipsychotic efficacy comparable with olanzapine (Patil et al., 2007).

Catalepsy is thought to reflect drug-induced suppression of the ability to initiate a behavioral response and is considered to be predictive of extrapyramidal side effects (Hoffman and Donovan, 1995). Despite differences in the intensity of the response, both the D2 antagonist haloperidol and the atypical D2/5-HT_{2A} receptor antagonist ziprasidone induced a dose- and time-dependent catalepsy in rats. Although initial studies with papaverine found no evidence of catalepsy (Siuciak et al., 2006b), its relatively poor pharmaceutical properties limited the ability to dose above its CAR ED_{50}. Although TP-10 was able to produce catalepsy, this response was neither dose- nor time-dependent, nor did it reach the intensity observed with either D2 antagonist. Thus, even at high and sustained levels of PDE10A inhibition, the ability of the animals to initiate a motor response was only moderately suppressed.

The similarities and differences between the behavioral effects of the PDE10A inhibition and D2 receptor blockade may be explained by contrasting their effects on striatal function. The striatum is the primary site of midbrain dopaminergic and cortical glutamatergic input to the basal ganglia, a subcortical circuit that functions as a cortical feedback loop. Within the striatum, cortically driven response options are reinforced according to coincident dopaminergic regulation of two functionally opposed striatal projections referred to as the direct and indirect pathways (Cheer et al., 2007). Direct pathway MSNs selectively express D1 receptors positively coupled to adenylyl cyclase. Phasic, D1 receptor-mediated increases in cAMP enhance the activity of direct pathway MSN to facilitate ongoing behaviors. Although the indirect pathway functions to tonically inhibit behavior, the MSNs forming these projections express D2 receptors negatively coupled to adenylyl cyclase hence their activity is inhibited by dopamine (see Surmeier et al., 2007). Thus, appropriately timed increases in dopamine release can facilitate behavior by simultaneously enabling direct pathway activity and inhibiting indirect pathway activity. In contrast, behavioral patterns coincident with reduced dopaminergic signaling are deselected due to decreased direct pathway activity and increased indirect pathway activity.

Given the high level of expression of PDE10A in MSNs, it is reasonable to conclude that inhibition of the enzyme alters the signaling of indirect pathway neurons in a way similar to that of D2 antagonists, i.e., via an increase in cyclic nucleotides. This would account for the observation that both classes of compounds produce many similar behavioral effects. However, PDE10A is also expressed in direct pathway MSNs (Seeger et al., 2003; Coskran et al., 2006; Xie et al., 2006) predicting that PDE10A inhibitors will increase the activity of the direct pathway neurons as well. This is supported by the observation that PDE10A inhibition enhances the expression of both substance P and enkephalin, markers for the direct and indirect pathways, respectively (C. A. Strick and L. C. Jame, unpublished data). Given the opposing effects of the two systems on basal ganglia output, we hypothesized that the modest cataleptic effect of TP-10 may in fact be the result of PDE10A inhibition affecting both the indirect and direct pathways. Reports that behavioral supersensitivity and up-regulation of D2 receptors after chronic antipsychotic treatment are prevented by cotreatment with D1 agonists (Marin and Chase, 1993; Glavan et al., 2002) are consistent with this suggestion. Enhanced direct pathway activity after PDE10A inhibition may also explain the failure of TP-10 to improve PPI. D1 agonists reportedly disrupt PPI in mice (Ralph-Williams et al., 2002, 2003; M. J. Majchrzak and P. A. Seymour, unpublished data). Thus, direct pathway activation may counter any effect of PDE10A inhibition on PPI resulting from indirect pathway activation. Confirmation of this hypothesis may require evaluating the effects of PDE10A inhibitors on PPI in rats, which are reportedly less sensitive to the disruptive effects of D1 agonists (Ralph-Williams et al., 2003).

An additional, subtler, mechanism may also contribute to the apparent benign behavioral profile of PDE10A inhibitors. Both PDE10A inhibitors and D2 antagonists cause increases in dopamine turnover in the striatum, with the latter being attributed to an increase in the firing rate of midbrain dopaminergic neurons and in the rate of dopamine synthesis (Zetterström et al., 1986). The mechanism responsible for the effect of TP-10 on dopamine turnover is presently unknown, although alterations in striatonigral feedback secondary to increased striatal output are obvious candidates. Regardless of mechanism, inhibition of PDE10A does not directly prevent D2 receptor stimulation and therefore should leave dopaminergic neurotransmission largely intact. Thus, PDE10A inhibition may allow a more physiological response to phasic changes in dopamine release than can occur during D2 receptor blockade. This unique mechanism allows for the possibility of using PDE10A inhibitors to augment the clinical activity of low dose D2 receptor antagonist therapy. Although we have not investigated this possibility fully, we have reported that the nonselective PDE10A inhibitor papaverine can potentiate the cataleptic activity of haloperidol (Siuciak

et al., 2006b). Whether this will be observed with more selective agents such as TP-10 or how a PDE10A inhibitor will interact with an atypical agent awaits further study.

In summary, we propose that PDE10A inhibition tonically increases indirect pathway activity, accounting for an antidopaminergic profile that includes dampened locomotion, inhibition of CAR and activity in the rat auditory gating model. Projecting to patients with schizophrenia, the ability of PDE10A inhibitors to blunt the aberrant attribution of salience and improve sensory gating should reduce psychosis. Simultaneous activation of the indirect and direct pathway during PDE10A inhibition may account for the relatively weak cataleptic response of compounds such as TP-10. Thus, PDE10A inhibition may be less behaviorally disruptive than approaches targeting only one pathway. The discovery of a new class of PDE10A inhibitors exemplified by TP-10 and MP-10 provides an opportunity to further explore the physiology of PDE10A and the potential therapeutic utility of inhibiting this enzyme. The results of the present studies support the hypothesis that PDE10A inhibitors will provide a novel and potentially differentiated therapy for the treatment of schizophrenia and establish TP-10 as a research tool to further investigate the role of PDE10A in basal ganglia function.

References

American Psychiatric Association (2004) Practice guideline for the treatment of patients with schizophrenia, second edition. *Am J Psychiatry* **161:**1–56.

Braff DL and Light GA (2004) Preattentional and attentional cognitive deficits as targets for treating schizophrenia. *Psychopharmacology* **174:**75–85.

Cheer JF, Aragona BJ, Heien MLA, Seipel AT, Carelli RM, and Wightman RM (2007) Coordinated accumbal dopamine release and neural activity drive goal directed behavior. *Neuron* **54:**237–244.

Coskran TM, Morton DG, Menniti FS, Adamowicz WO, Kleiman RJ, Ryan AM, Strick CA, Schmidt CJ, and Stephenson DT (2006) Immunohistochemical localization of phosphodiesterase 10A, PDE10A, in multiple mammalian species. *J Histochem Cytochem* **54:**1205–1213.

Coyle JT (2006) Glutamate and schizophrenia: beyond the dopamine hypothesis. *Cell Mol Neurobiol* **26:**363–382.

Geyer MA, Krebs-Thomson K, Braff DL, and Swerdlow NR (2001) Pharmacological studies of prepulse inhibition models of sensorimotor gating deficits in schizophrenia: a decade in review. *Psychopharmacology (Berl)* **156:**117–154.

Geyer MA, Swerdlow NR, Mansbach RS, and Braff DL (1990) Startle response models of sensorimotor gating and habituation deficits in schizophrenia. *Brain Res Bull* **25:**485–498.

Glavan G, Sket D, and Zivin M (2002) Modulation of neuroleptics activity of 9,10-didehydro-N-methyl-(2-propyl)-6-methyl-8-aminomethylergoline bimaleinate (LEK-8829) by D1 intrinsic activity in hemi-parkinsonian rats. *Mol Pharmacol* **61:**360–368.

Gottesman II and Gould TD (2003) The endophenotype concept in psychiatry: etymology and strategic intentions. *Am J Psychiatry* **160:**636–645.

Green MF (1996) What are the functional consequences of neurocognitive deficits in schizophrenia? *Am J Psychiatry,* **153:**321–330.

Guillin O, Abi-Dargham A, and Laruelle M (2007) Neurobiology of dopamine in schizophrenia. *Int Rev Neurobiol* **78:**1–39.

HajósM, Hurst RS, Hoffman WE, Krause M, Wall TM, Higdon NR, and Groppi VE (2005) The selective alpha7 nicotinic acetylcholine receptor agonist PNU-282987 [N-[(3R)-1-azabicyclo[2.2.2]oct-3-yl]-4-chlorobenzamide hydrochloride] enhances GABAergic synaptic activity in brain slices and restores auditory gating deficits in anesthetized rats. *J Pharmacol Exp Ther* **312:**1213–1222.

Henry SA, Lehmann-Masten V, Gasparini F, Geyer MA, and Markou A (2002) The mGluR5 antagonist MPEP, but not the mGluR2/3 agonist LY314582, augments PCP effects on prepulse inhibition and locomotor activity. *Neuropharmacology* **43:**1199–1209.

Hoffman DC and Donovan H (1995) Catalepsy as a rodent model for detecting antipsychotic drugs with extrapyramidal side-effect liability. *Psychopharmacology (Berl)* **120:**128–133.

Imre G, Salomons A, Jongsma M, Fokkema DS, Den Boer JA, and Ter Horst GJ (2006) Effects of the mGluR2/3 agonist LY379268 on ketamine-evoked behaviors and neurochemical changes in the dentate gyrus of the rat. *Pharmacol Biochem Behav* **84:**392–399.

Institute of Laboratory Animal Resources (1996) *Guide for the Care and Use of Laboratory Animals* 7th ed. Institute of Laboratory Animal Resources, Commission on Life Sciences, National Research Council, Washington DC.

Javitt DC (2007) Glutamate and schizophrenia: phencyclidine, N-methyl-D-aspartate receptors and dopamine-glutamate interactions. *Int Rev Neurobiol* **78:**69–108.

Jentsch JD and Roth RH (1999) The neuropsychopharmacology of phencyclidine: from NMDA receptor hypofunction to the dopamine hypothesis of schizophrenia. *Neuropsychopharmacology* **20:**201–225.

Johnson KM and Jones SM (1990) Neuropharmacology of phencyclidine: basic mechanisms and therapeutic potential. *Annu Rev Pharmacol Toxicol* **30:**707–750.

Kapur S (2003) Psychosis as a state of aberrant salience: a framework linking biology, phenomenology, and pharmacology in schizophrenia. *Am J Psychiatry* **160:**13–23.

Keefe RS, Bilder RM, Davis SM, Harvey PD, Palmer BW, Gold JM, Meltzer HY, Green MF, Capuano G, Stoup TS, et al. (2007) Neurocognitive effects of antipsychotic medications in patients with chronic schizophrenia in the CATIE trial. *Arch Gen Psychiatry* **64:**633–647.

Krause M, Hoffman WE, and Hajos M (2003) Auditory sensory gating in hippocampus and reticular thalamic neurons in anesthetized rats. *Biol Psychiatry* **53:**244–253.

Laruelle M, Kegeles LS, and Abi-Dargham A (2003) Glutamate, dopamine and schizophrenia: from pathophysiology to treatment. *Ann Natl Acad Sci* **1003:**138–158.

LonzeBE and Ginty DD (2002) Function and regulation of CREB family transcription factors in the nervous system. *Neuron* **35:**605–623.

Mackin P, Bishop D, Watkinson H, Gallagher P, and Ferrier IN (2007) Metabolic disease and cardiovascular risk in people treated with antipsychotics in the community. *Br J Psych* **191:**23–29.

Marin C and Chase TN (1993) Dopamine D1 receptor stimulation but not dopamine D2 receptor stimulation attenuates haloperidol-induced behavioral sensitivity and receptor up-regulation. *Eur J Pharmacol* **231:**191–196.

Menniti FS, Chappie TA, Humphrey JM, and Schmidt CJ (2007) Phosphodiesterase 10A (PDE10A) inhibitors: a novel approach to the treatment of the symptoms of schizophrenia. *Curr Opin Invest Drug* **8:**54–59.

Newcomer JW (2005) Second generation (atypical) antipsychotics and metabolic effects: a comprehensive literature review. *CNS Drugs* **19 (Suppl 1):**1–93.

Ouagazzal AM, Jenck F, and Moreau JL (2001) Drug-induced potentiation of prepulse inhibition of acoustic startle reflex in mice: a model for detecting antipsychotic activity? *Psychopharmacology (Berl)* **156:**273–283.

Patil ST, Zhang L, Martenyi F, Lowe SL, Jackson KA, Andreev BV, Avedisova AS, Bardenstein LM, Gurovich IY, Morozova MA, et al. (2007) Activation of mGluR2/3 receptors: a new approach to treat schizophrenia: a randomized phase 2 clinical trial. *Nat Med* **13:**1102–1107.

Paylor R and Crawley JN (1997) Inbred strain differences in prepulse inhibition of the mouse startle response. *Psychopharmacology* **132:**169–180.

Paxinos G and Watson C (1986) *The Rat Brain in Stereotactic Coordinates,* Academic Press, San Diego.

Ralph-Williams RJ, Lehmann-Masten V, Otero-Corchon, Low MJ, and Geyer MA (2002) Differential effects of direct and indirect dopamine agonists on prepulse inhibition: a study in D1 and D2 knock-out mice. *J Neurosci* **22:**9604–9611.

Ralph-Williams RJ, Lehmann-Masten V, and Geyer MA (2003) D1 rather than D2 receptors disrupt prepulse inhibition of startle in mice. *Neuropsychopharmacology* **28:**108–118.

Seeger TF, Bartlett B, Coskran TM, Culp JM, James LC, Krull DL, Lanfear J, Ryan AM, Schmidt CJ, Strick CA, et al. (2003) Immunohistochemical localization of PDE10A in the rat brain. *Brain Res* **985:**113–126.

Siuciak JA, McCarthy SA, Chapin DS, Fujiwara RA, James LC, Williams RD, Stock JL, McNeish JD, Strick CA, Menniti FS, et al. (2006a) Genetic deletion of the striatum-enriched phosphodiesterase PDE10A: evidence for altered striatal function. *Neuropharmacology* **51:**374–385.

Siuciak JA, Chapin DS, Harms JF, Lebel LA, James LC, McCarthy SA, Chambers LK, Shrikehande A, Wong SK, Menniti FS, et al. (2006b) Inhibition of the striatum-enriched phosphodiesterase PDE10A: a novel approach to the treatment of psychosis. *Neuropharmacology* **51:**386–396.

Strick CA, Schmidt CJ, and Menniti FS (2006) PDE10A: a striatum enriched, dual-substrate phosphodiesterase, in *Phosphodiesterases in Health and Disease* (Francis S, Housley M, and Beavo J eds), pp 237–254, CRC Press, Boca Raton, FL.

Surmeier DJ, Ding J, Day M, Wang Z, and Shen W (2007) D1 and D2 dopamine receptor modulation of striatal glutamatergic signaling in striatal medium spiny neurons. *Trends Neurosci* **30:**228–235.

Verhoest PR, Helal CJ, Hoover DJ, and Humphrey JM (2006) inventors; Pfizer Products, Inc., assignee. Heteroaromatic quinoline compounds as phosphodiesterase inhibitors, their preparation, pharmaceutical compositions, and use in therapy. World patent WO 2006072828. 2006 Jul 13.

Wadenberg M-LG and Hicks PB (1999) The conditioned avoidance response test re-evaluated: is it a sensitive test for the detection of potentially atypical antipsychotics? *Neurosci Biobehav Rev* **23:**851–862.

Xie Z, Adamowicz WO, Eldred WD, Jakowski AB, Kleiman RJ, Morton DG, Stephenson DT, Strick CA, Williams RD, and Menniti FS (2006) Cellular and subcellular localization of PDE10A, a striatal-specific phosphodiesterase. *Neuroscience* **139:**597–607.

ZetterströmT, Sharp T, and Ungerstedt U (1986) Effect of D1 and D2 receptor selective drugs on dopamine release and metabolism in rat striatum in vivo. *Naunyn Schmiedebergs Arch Pharmacol* **334:**117–124.

Address correspondence to: Dr. Christopher J. Schmidt, Neuroscience, Pfizer Global Research and Development, Pfizer, Inc., Eastern Point Road, Groton, CT 06340. E-mail: Christopher.j.schmidt@pfizer.com